Planetary and Space Science 75 (2013) 96–104

Contents lists available at SciVerse ScienceDirect

Planetary and Space Science

journal homepage: www.elsevier.com/locate/pss

Impact disruption of primordial planetesimals

M. Gabriela Parisi [a,b,*,1]

[a] Instituto Argentino de Radioastronomía (CCT-La Plata, CONICET), C.C. No. 5, 1894 Villa Elisa, Prov. de Buenos Aires, Argentina
[b] Facultad de Ciencias Astronómicas y Geofísicas, Universidad Nacional de La Plata, La Plata, Prov. de Buenos Aires, Argentina

ARTICLE INFO

Article history:
Received 14 January 2012
Received in revised form
27 August 2012
Accepted 24 September 2012
Available online 29 October 2012

Keywords:
Solar System formation
Planetesimals
Accretion

ABSTRACT

It is usually assumed that 1–10-km-sized planetesimals are formed through coagulation processes and continue to agglomerate via pairwise mergers. However, recent models of planetesimal formation suggest that planetesimals of 100–1000 km were produced directly from small solid particles without experiencing accretion through intermediate sizes. At present, if planetesimals were born small or big is a matter of debate. We investigate if planetesimals in the range 10–1000 km suffer growth or disruption as they collide. The collisional energy required for disruption is computed as a function of the planetesimals radius and velocity in terms of their orbital semiaxis and eccentricity. We obtain that growth of planetesimals of $\sim 10-100$ km in the asteroid belt and the Kuiper belt requires eccentricities much lower than what we observe today. Simulations of accretion in the terrestrial and giant planets region show that planetesimals of 10–100 km reach values of the eccentricity which lie at the disruption eccentricity limit obtained in this work. We obtain that planetesimals growth requires a very cold disk during all the accretionary process, which seems to be difficult to achieve. We conclude that large planetesimals may be formed either invoking modern scenarios of gravitational instability or by accreting small bodies only. Planetesimals of intermediate sizes would then be the result of disruption events. We obtain that accretion requires an impactor target mass ratio smaller than 0.1–0.01. This implies that the exponent q of the power law mass distribution of bodies must be greater than two during all the planetary formation process. However, if during oligarchic growth a bimodal mass distribution of small and large bodies exists, the mass distribution of small bodies allows $q<2$ provided the mass ratio between the largest body of such distribution and the smallest body of the distribution of large planetesimals is smaller than $\sim 0.1-0.01$.

1. Introduction

It is usually accepted that terrestrial planets and cores of giant planets are formed through accretion of planetesimals. Several mechanisms of planetesimal formation have been proposed, beginning with classical analysis of gravitational instability in a dense layer of small particles that settled to the midplane of the solar nebula (Safronov, 1969; Goldreich and Ward, 1973). The radius of the primordial planetesimals was obtained as the largest body that can condense out of a gravitationally unstable cold disk while conserving its internal angular momentum and was estimated to be ~ 1 km. This mechanism in its simplest form is not viable due to the generation of turbulence by shear in the layer (Weidenschilling, 1980). Very recently, variations of gravitational instability have been proposed, involving collapse of concentrations of particles produced by a streaming instability (Youdin and Goodman, 2005) or turbulence (Johansen et al., 2007). These models predicts that primordial planetesimals with sizes in the range 100–1000 km were produced directly from small solid particles without experiencing accretion through intermediate sizes. Johansen et al. (2012) found efficient formation of gravitational bound clumps formed in filaments caused by the streaming instability, with a range of masses corresponding to contracted radii from 100 to 400 km when applied to the asteroid belt and from 150 to 730 km when scaled to the Kuiper belt.

The most commonly considered scenario of planetesimal formation is the coagulation of aggregate bodies in collisions driven by differential gas drag (Weidenschilling, 1997). Dust sediments towards the midplane of the solar nebula and starts to collide with each other at low velocities. The particles eventually stick together through electrostatic forces, forming larger fractal aggregates (e.g., Blum et al., 2000; Paszun and Dominik, 2009). Further collisions make these aggregates more compact forming larger objects. During the coagulation process, gas drag dominates the behavior of these objects since the escape velocity

* Correspondence address: Instituto Argentino de Radioastronomía (CCT-La Plata, CONICET), C.C. No 5, 1894 Villa Elisa, Prov. de Buenos Aires, Argentina.
Tel./fax: +54 221 4254909.
E-mail addresses: gparisi@iar-conicet.gov.ar, gabriela_parisi@hotmail.com
[1] Member of the Carrera del Investigador Científico, Consejo Nacional de Investigaciones Científicas y Técnicas (CONICET), Argentina.

0032-0633/$ - see front matter © 2012 Elsevier Ltd. All rights reserved.
http://dx.doi.org/10.1016/j.pss.2012.09.013

on their surface is less than their drag-induced radial velocity. When these objects are of the order of ~ 1 km in size, the escape velocity on their surface turns higher than the drag-induced radial velocity (Weidenschilling, 1997). Then, gravity starts to dominate the behavior of the system. It is usually assumed that the so-called planetesimals continue to agglomerate via pairwise mergers. The formation of km-sized planetesimals by coagulation has the disadvantage that it requires low relative velocities between colliding aggregates, which does not occur in the centimeter-to-meter size range. Moreover, Ida et al. (2008) have shown that turbulent gas causes high, disruptive collision speed even between much larger bodies. Another problem with forming planetesimals by coagulation is that it takes very long time, while meteoritic constraints show that large, differentiated planetesimals must form within a million years to heat by decay of ^{26}Al (Bizzarro et al., 2005).

Planetesimals cannot be observed directly in protostellar disks, and the size of the primordial planetesimals in the Solar System remains a matter of debate (Morbidelli et al., 2009; Weidenschilling, 2011). Most simulations of accretion start with planetesimals of the classical size of 1–10 km. There is no reason to prefer this size, although it has become a standard in calculations of planetary accretion. The concept of km-sized planetesimals has persisted, and remains the default option for the initial condition in most calculations of planetary accretion.

Planetary accretion has been investigated mainly by solving the coagulation equation of planetesimals under the particle-in-a-box approximation (e.g., Nakagawa et al., 1983; Weidenschilling et al., 1997). Evolution of the mass distribution of planetesimals is calculated using the collision probability given as a function of mass and velocity of planetesimals, coupling with the calculation of the evolution of the velocity distribution using the kinetic theory. The complementary method to the statistical approach is N-body simulations. This approach is suitable for the study of the late stage of planetary accretion (e.g., Ida and Makino, 1992).

In most calculations of accretion, it is assumed that two planetesimals always accrete when they contact (e.g., Kokubo and Ida, 2000). The relative velocity between planetesimals is a function of their orbital eccentricity and inclination, which increases as a result of mutual perturbations and stirring by planetary embryos and decreases by gas drag and inelastic collisions (e.g., Inaba et al., 2001). Although the lack of collisional fragmentation or rebound seems to make no significant change in the growth mode of protoplanets (Kokubo and Ida, 2000; Inaba et al., 2001), we wonder if really planetesimals accrete or if they disrupt as they collide.

In this paper, we investigate if planetesimals suffer growth or disruption when collisions take place. In Section 2, the disruption radius of planetesimals is calculated as a function of their orbital semiaxes for different values of the orbital eccentricity. The results are presented in Section 3 and the discussion of the results in Section 4. In Section 5, we study the formation of large planetesimals by the accretion of small particles and Section 6 contains the concluding remarks.

2. Calculation of the disruption radius of planetesimals

Whether a collision between an impactor and a target results in growth or erosion of the target depends on the energy of the impact and the mass, radius, and strength of the target. The energy necessary to disrupt the target can be divided into that necessary to overcome its material strength S_t (energy/unit mass), and that necessary to overcome its gravity. If m_i is the mass of the impactor and m_t is the mass of the target, the energy required at impact to result in disruption of the target is then given by (Stevenson et al., 1986)

$$\frac{1}{2}m_i v_{col}^2 \geq m_t S_t + \frac{3}{5}\frac{Gm_t^2}{\gamma R}, \tag{1}$$

where v_{col} is the collision speed, R is the radius of the target and γ is a parameter which specifies the fraction of collisional kinetic energy that goes into fragment kinetic energy and is estimated to be ~ 0.1 (e.g., Farinella and Davis, 1996; Davis et al., 1989). The speed of the fragments is critical when the target has a gravity field. Fragments moving slower than the local escape speed re-accumulate to form rubber pile structures.

We investigate whether a collision on a primary body would result in disruption or in a rubber pile structure. In computing Eq. (1), the collision speed is given by

$$v_{col}^2 = v_e^2 + v_{inf}^2, \tag{2}$$

where v_e is the escape velocity from the point of contact and v_{inf} is the typical approach velocity of the two objects at a distance large compared to the Hill sphere of the target. The approach velocity is given by (Lissauer and Stewart, 1993; Morbidelli et al., 2009)

$$v_{inf}^2 = v_k^2\left(\frac{5}{4}e^2 + i^2\right), \tag{3}$$

where v_k is the Keplerian velocity, e the mean orbital eccentricity and i the mean orbital inclination of the objects. We take $e = 2i$ (Stern, 1996a,b).

We assume that m_t is a spherical body with bulk density ρ_t, i.e., $m_t = 4/3\pi\rho_t R^3$. The disruption radius is then computed through Eq. (1) using Eqs. (2) and (3) for three values of the impactor mass, $m_i = m_t$, $m_i = 0.1m_t$, and $m_i = 0.01m_t$. In calculations of planetary accretion where complete accretion is assumed, the orbital eccentricity of planetesimals increases above 0.01 (e.g., Kokubo and Ida, 2000; Inaba et al., 2001). Then, in order to investigate if an eccentricity above 0.01 is consistent with complete accretion, we compute Eq. (3) for $e = 0.01$, 0.03, 0.05, and 0.1. The dependence of the disruption radius with the orbital semiaxis a is given through the Keplerian speed in Eq. (3).

3. Results

3.1. Inner Solar System

The disruption radius of primordial planetesimals was computed for orbital semiaxes a between 0.4 and 3 AU. In computing m_t, we assume bulk densities of 3 g cm^{-3} and 5 g cm^{-3}. We take $S_t \sim 3 \times 10^7$ erg g^{-1} for typical objects and $S_t \sim 3 \times 10^8$ erg g^{-1} for very strong objects. Objects with $\rho_t = 5$ g cm^{-3} and $S_t = \times 10^8$ erg g^{-1} are unusual, but we include this case for comparison.

The disruption radius as a function of the orbital semiaxis for $m_i = m_t$ is displayed in Fig. 1. For $\rho_t = 3$ g cm^{-3} and $S_t = 3 \times 10^7$ erg g^{-1} with $e \sim 0.01$, disruption of 100 (200)-km-sized bodies occurs at 1.6 (0.4) AU while disruption of 70 km-sized bodies at 3 AU. For $\rho_t = 5$ g cm^{-3} and $S_t = 3 \times 10^8$ erg g^{-1} with $e \sim 0.01$, disruption of 70 (150)-km-sized bodies occurs at 1 (0.4) AU while disruption of 10 km-sized planetesimals at ~ 2.2 AU. At 0.4–3 AU, 200-km-sized planetesimals are disrupted if $e \sim 0.03$ while 1000-km-sized bodies are disrupted if e ~ 0.1 for any value of the density and strength.

The disruption radius as a function of the orbital semiaxis for $m_i = 0.1m_t$ is displayed in Fig. 2. For $\rho_t = 3$ g cm^{-3} and $S_t = 3 \times 10^7$ erg g^{-1}, disruption of 60 (200)-km-sized bodies occurs at 3 (0.4) AU if $e \sim 0.03$, while if $e \sim 0.01$, disruption of 10 (50)-km-sized bodies occurs at ~ 2 (0.4) AU. For $\rho_t = 5$ g cm^{-3} and $S_t = 3 \times 10^8$ erg, disruption of 10 (100)-km-sized bodies occurs at 2 (0.4) AU if $e \sim 0.03$. One hundred and fifty kilometer-sized bodies are disrupted at 0.4–3 AU if $e \sim 0.1$ for any value of the density and strength.

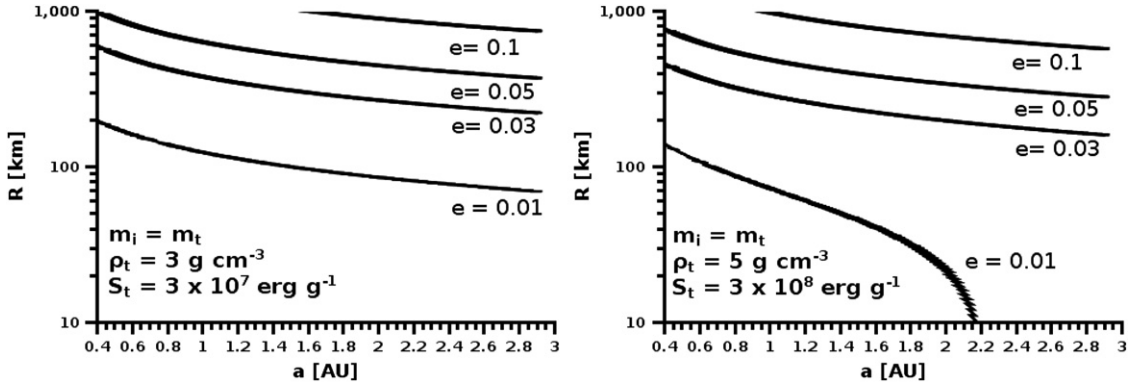

Fig. 1. Target disruption radius as function of the orbital semiaxis in the inner Solar System. The upper curve is for a mean eccentricity $e=0.1$, while the lower curve is for $e=0.01$. Intermediate curves correspond to $e=0.03$ and $e=0.05$. *Right*: Target density $\rho_t = 5$ g cm^{-3} and strength $S_t = 3\times10^8$ erg g^{-1}. *Left*: Target density $\rho_t = 3$ g cm^{-3} and strength $S_t = 3\times10^7$ erg g^{-1}. The impactor mass m_i is equal to the target mass m_t.

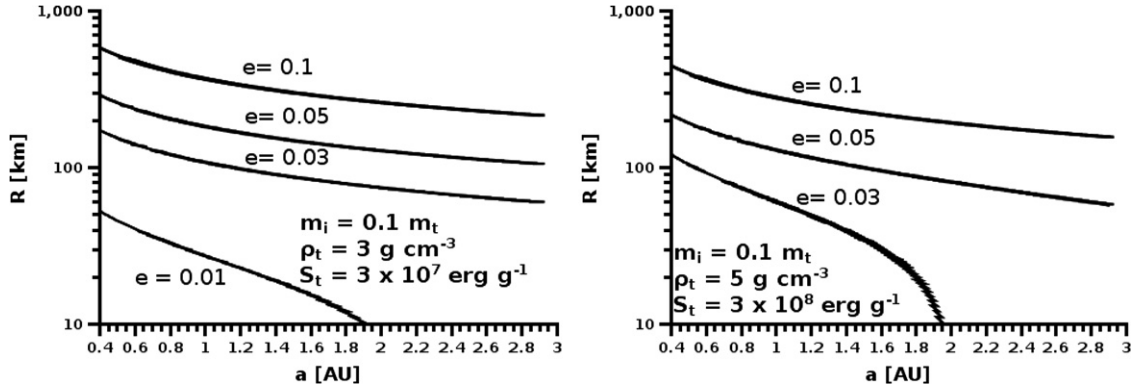

Fig. 2. The same than in Fig. 1 for $m_i=0.1m_t$.

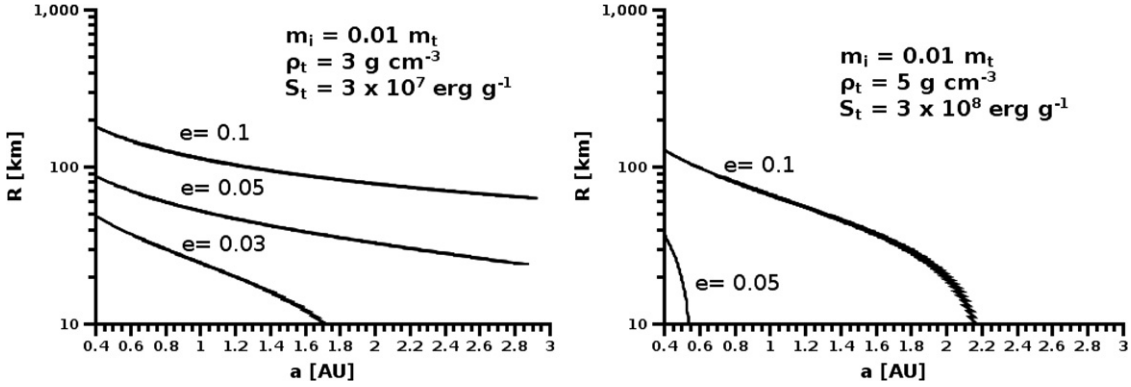

Fig. 3. The same than in Fig. 1 for $m_i=0.01m_t$.

The disruption radius as a function of the orbital semiaxis for $m_i=0.01m_t$ is displayed in Fig. 3. For $\rho_t = 3$ g cm^{-3} and $S_t = 3\times10^7$ erg g^{-1}, disruption of 10 (50) km-sized bodies occurs at 1.7 (0.4) AU if $e\sim0.03$, while 30 (100)-km-sized bodies are disrupted at 3 (0.4) AU if e is ~0.05. For $\rho_t = 5$ g cm^{-3} and $S_t = 3\times10^8$ erg g^{-1}, disruption of 10 (100)-km-sized bodies occurs at 2.2 (0.4) AU if $e\sim0.1$.

3.2. Outer Solar System

The disruption radius was computed for orbital semiaxes a between 2.5 and 60 AU. In computing m_t, we assume bulk densities of 0.5 g cm^{-3}, 1 g cm^{-3}, and 2 g cm^{-3}. We take $S_t\sim3\times10^6$ erg g^{-1} for ices and 3×10^4 erg g^{-1} for objects mechanically weak like snow.

The disruption radius as a function of the orbital semiaxis for $m_i=m_t$ is displayed in Fig. 4. For $\rho_t = 0.5$ g cm^{-3} and $S_t = 3\times10^4$ erg g^{-1}, disruption of 40 (200)-km-sized bodies occurs at 60 (2.5) AU if e is ~0.01. For $\rho_t = 1$ g cm^{-3} and $S_t = 3\times10^6$ erg g^{-1}, disruption of 30 (120)-km-sized bodies occurs at 60 (2.5) AU if e is ~0.01. For $\rho_t = 2$ g cm^{-3} and $S_t = 3\times10^6$ erg g^{-1}, disruption of 20 (100)-km-sized bodies occurs at 60 (2.5) AU if e is ~0.01. One thousand kilometer-sized bodies are disrupted at 2.5 AU and 300 km-sized bodies are disrupted at 60 AU if $e\sim0.1$ for any value of the density and strength.

The disruption radius as a function of the orbital semiaxis for $m_i=0.1m_t$ is displayed in Fig. 5. For $\rho_t = 0.5$ g cm^{-3} and

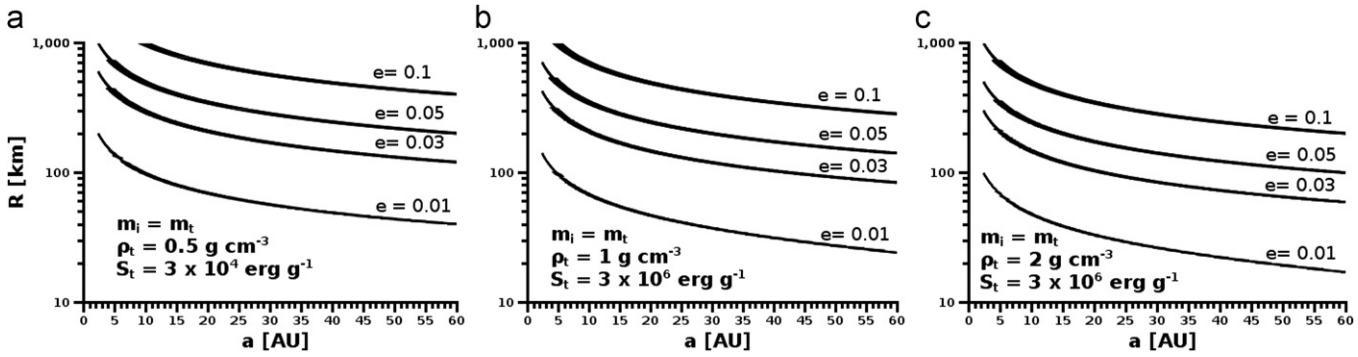

Fig. 4. Target disruption radius as function of the orbital semiaxis in the outer Solar System. The upper curve is for a mean eccentricity $e=0.1$, while the lower curve is for $e=0.01$. Intermediate curves correspond to $e=0.03$ and $e=0.05$. (a) Target density $\rho_t=0.5$ g cm^{-3} and strength $S_t=3\times10^4$ erg g^{-1}. (b) Target density $\rho_t=1$ g cm^{-3} and strength $S_t=3\times10^6$ erg g^{-1}. (c) Target density $\rho_t=2$ g cm^{-3} and strength $S_t=3\times10^6$ erg g^{-1}. The impactor mass m_i is equal to the target mass m_t.

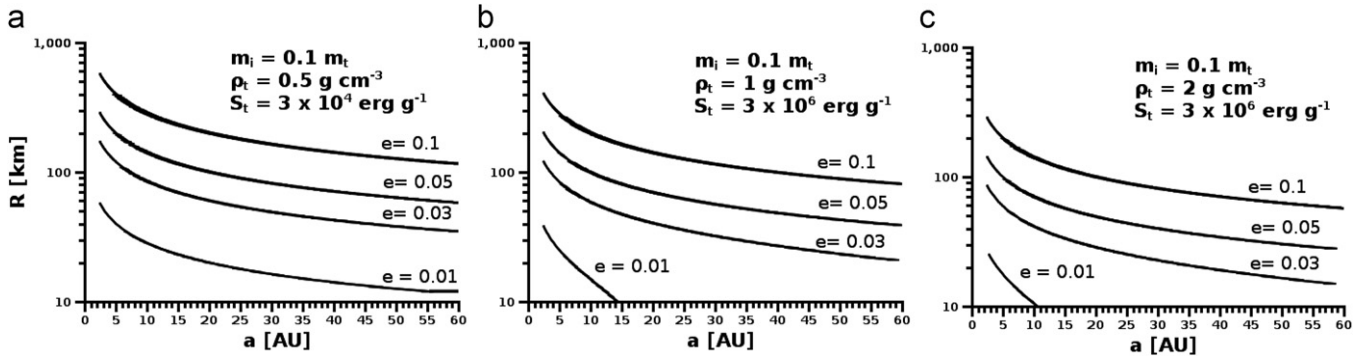

Fig. 5. The same than in Fig. 4 for $m_i=0.1m_t$.

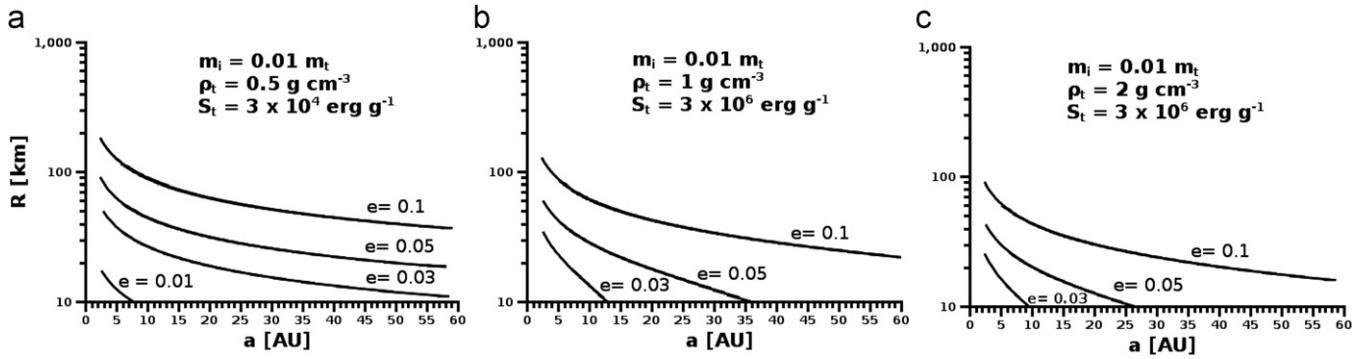

Fig. 6. The same than in Fig. 4 for $m_i=0.01m_t$.

$S_t=3\times10^4$ erg g^{-1}, disruption of 10 (50)-km-sized bodies occurs at 60 (2.5) AU if e is ~0.01. For $\rho_t=1$ g cm^{-3} and $S_t=3\times10^6$ erg g^{-1}, disruption of 10 (40)-km-sized bodies occurs at 15 (2.5) AU if e is ~0.01 while disruption of 30 (100)-km-sized bodies occurs at 60 (2.5) AU if e is ~0.03. For $\rho_t=2$ g cm^{-3} and $S_t=3\times10^6$ erg g^{-1}, disruption of 10 (30)-km-sized bodies occurs at 10 (2.5) AU if e is ~0.01 while disruption of 30 (100)-km-sized bodies occurs at 60 (2.5) AU if e is ~0.03. Three hundred kilometer-sized bodies are disrupted at 2.5 AU while 100 km-sized bodies are disrupted at 60 AU if $e\sim0.1$ for any value of the density and strength.

The disruption radius as a function of the orbital semiaxis for $m_i=0.01m_t$ is displayed in Fig. 6. For $\rho_t=0.5$ g cm^{-3} and $S_t=3\times10^4$ erg g^{-1}, disruption of 10 (20)-km-sized bodies occurs at 7 (2.5) AU for $e\sim0.01$ while disruption of 10 (50)-km-sized bodies occurs at 60 (2.5) AU if e is ~0.03. For $\rho_t=1$ g cm^{-3} and $S_t=3\times10^6$ erg g^{-1}, disruption of 10 (30)-km-sized bodies occurs at 13 (2.5) AU if e is ~0.03 while disruption of ~30 (100)-km-sized bodies occurs at 60 (2.5) AU if e is 0.1. For $\rho_t=2$ g cm^{-3} and $S_t=3\times10^6$ erg g^{-1}, disruption of 10 (30)-km-sized bodies occurs at 10 (2.5) AU if e is ~0.03 while disruption of 20 (100)-km-sized bodies occurs at 60 (2.5) AU if e is 0.1.

4. Discussion

4.1. Terrestrial planets region

We obtain that for typical bulk densities and strength in the inner Solar System, collisions between 70 (200)-km-sized planetesimals at 3 (0.4) AU result in disruption if the mean eccentricity e is ~0.01. But if the mass of the impactor is much less than the mass of the target, disruption of targets of that size requires $e\sim0.05-0.1$. Growth of ~10-km-sized planetesimals within ~2.5 AU requires $e<0.003$ if the collisions are between objects of similar size and $e<0.03$ if the impactor target mass ratio is very small.

The growth of 1–10 km-sized planetesimals to larger objects does not seem to be guaranteed. Ida et al. (2008) found the equilibrium values of the eccentricities of small planetesimals during the initial phase of the accretion process balancing the stirring effect of a turbulent disk with the damping effects due to gas drag and mutual collisions. They found that bodies of 1–10 km in size reach equilibrium values for e of $\sim 0.001-0.002$ at 1 AU. This value of e is very close to the e required for the disruption of such bodies in this work ($e \sim 0.003$).

Kokubo and Ida (2000) and Inaba et al. (2001) carried out simulations of accretion at later stages of the accretionary epoch. In Figure 5 of Inaba et al. (2001) and in Figure 5 of Kokubo and Ida (2000), the eccentricity reaches a maximum value of ~ 0.02 for $\sim$200-km−sized objects at 1 AU. In simulations where fragmentation is included (Wetheril and Stewart, 1993; Ohtsuki et al., 2002), the maximum value of e for objects of that size is ~ 0.03. Then, in simulations with and without fragmentation, the maximum eccentricity acquired by 200-km-sized objects at 1 AU is $\sim 0.02-0.03$. However, we obtain from Fig. 1 that collisions between $\sim$200-km−sized objects result in disruption if $e \sim 0.02$ at 1 AU. We may then conclude, that the maximum value of the eccentricity acquired by 200-km-sized objects lies at their disruption limit.

One of the main problems is that no one knows precisely the energy delivered by the impactor required for catastrophic disruption of the target and there have been many different estimates. In any case, the impact velocity of small and large planetesimals at different stages of the accetionary epoch seems to reach values which are close to their disruption velocity limit. Growth of planetesimals smaller than 200 km is then questionable.

4.2. Asteroid belt

The main result is that disruption of targets of ~ 100 km in radius requires $e \sim 0.1$ in the inner, main, and outer asteroid belt. Growth of 10-km-sized planetesimals requires $e < 0.03-0.05$ in the inner and main asteroid belt and $e < 0.01-0.03$ in the outer asteroid belt.

The present impact velocities in the asteroid belt are ~ 5 km s^{-1}, i.e., $e \sim 0.2$ (e.g., Bottke et al., 1994, 2005; Farinella and Davis, 1992; Manley et al., 1998). Bottke et al. (2005) suggest that the present eccentricities were acquired prior to the formation of Jupiter, when planetary embryos excited asteroids velocities to ~ 6 km s^{-1}. They found that most asteroids with radius greater than 60 km are primordial and that smaller asteroids are byproducts of fragmentation events. However, we find that asteroids with radius of ~ 100 km striking with smaller bodies are disrupted if the impact velocity is greater than ~ 2 km s^{-1} ($e = 0.1$). Then, asteroids of ~ 100 km in radius are therefore likely to be suffering erosion and disruption today and cannot be primordial if the present eccentricities are primordial. The difference between the results of Bottke et al. (2005) and our results, possibly resides in the uncertainties in the critical impact energy required for catastrophic disruption of the target and how it varies with velocity (Benz, 2000; Asphaug et al., 2002).

Our results suggest that either the primordial eccentricities in the asteroid belt were much lower than what we observe today, or a larger primordial population of asteroids with radius much higher than ~ 100 km were produced directly from small solid particles without experiencing accretion through intermediate sizes.

The present size frequency distribution of bodies in the asteroid belt has an excess of bodies with radius 50 km relative to a simple power law. Morbidelli et al. (2009) found that the present size frequency distribution of bodies in the asteroid belt cannot be reproduce by accretion from an initial population of km-sized planetesimals. They concluded that asteroids were born big, suggesting that the minimal radius of the planetesimals was ~ 50 km. However, Weidenschilling (2011) found that the requisite size frequency distribution of asteroids can be produce from an initial population of sub-km planetesimals, smaller than the usual assumption of km-sized bodies, provided the velocities are very small. However, once planetary embryos are formed, the velocities are excited. Kobayashi et al. (2010) have shown that the stirring of random velocities of planetesimals by embryos makes collisions between planetesimals destructive and that the resulting fragments are ground down by successive collisions being the smallest fragments removed by inward drift due to gas drag.

Growth of planetesimals requires low eccentricities during all the accretionary epoch which seems to be a difficult issue. An initial planetesimal size as large as 100 km seems to solve this problem provided the eccentricities were lower than 0.1 during all the accretionary process. But if planetary embryos excite eccentricities above 0.1, the primordial planetesimals size should have been much larger than 100 km.

4.3. Giant planets region

In the giant planets region, collisions among 20–100-km-sized icy planetesimals and 60–200-km-sized snowy planetesimals result in disruption if the mean eccentricity e is ~ 0.01. But if the mass of the impactor is much less than the mass of the target, disruption of icy and snowy targets of 20 km requires $e \sim 0.05$ and ~ 0.03, respectively. Growth of planetesimals of ~ 10 km in the outer Solar System requires $e < 0.01-0.03$ for snow and $e < 0.01-0.05$ for ices, depending on the impactor and target mass ratio.

Thommes et al. (2003) found that as planetary embryos grow, gravitational stirring of planetesimals by embryos in the outer Solar System enhances random eccentricities of planetesimals up to 0.1–0.2. This values of the eccentricities are much higher than the values obtained for the disruption of planetesimals in this work.

Goldreich et al. (2004) suggested that if Uranus and Neptune were formed at their present locations, they grew by accreting bodies that were smaller than 1 km. They stated that if the accreted bodies had been bigger than 1 km, they would not have collided with each other sufficiently frequently to damp their speeds, which are stirred by planetary embryos. Accretion of such hot bodies would have taken longer than the age of the Solar System. They suggested that Uranus and Neptune would excite the velocity dispersion of these bodies to such extent that they would shatter when they collided, thereby creating much smaller bodies with smaller random velocities, which accelerates the accretion rate. However, Goldreich et al. (2004) neglected gas drag. Small planetesimals experience stronger damping of random velocities, forming a thinner disk and thus increasing the accretion rate. But in a laminar gas, small planetesimals are also subject to faster orbital decay due to gas drag, which depletes the planetesimal surface density at a given location in the disk more rapidly. However, turbulent gas can excite large scale pressure bumps, in which stochastic forcing by the magnetic tension on short timescales creates zonal flow structures with lifetimes of several tens of orbits, which are capable of slowing down or even stopping the radial drift (e.g., Johansen et al., 2009).

Benvenuto et al. (2009) computed the formation of all giant planets in an inner compact configuration in the framework of the Nice model (Tsiganis et al., 2005). They computed random velocities assuming the equilibrium between the gravitational perturbations due to the embryo and the dissipation due to gas drag. The accretion rate of small bodies increases due to the damping of their random velocities. They considered a size of the

accreted planetesimals in the range 30 m to 100 km assuming that planetesimals smaller than 20 m cannot be efficiently accreted due to orbital decay by gas drag. However, Benvenuto et al. (2009) neglected stirring by neighboring embryos and collisional fragmentation among planetesimals. Kobayashi et al. (2010) obtained that collisions between planetesimals are destructive and that the resulting fragments are ground down by successive collisions. They obtained that the smallest fragments are then removed by inward drift to gas drag, collisional disruption depletes the planetesimal disk and inhibits embryo growth. Then, embryo growth from an initial planetesimal size larger than 100 km would be required. However, if the gas is turbulent, large scale pressure bumps might stop the radial drift allowing, in principle, embryo growth from smaller bodies.

4.4. Kuiper belt

In the Kuiper belt, 20–40-km-sized snowy and icy bodies are disrupted if e is ~ 0.01. If the impactor mass is much less than the target mass, disruption of targets of that size occurs if $e \sim 0.03$ for snow and 0.1 for ice. Growth of 10-km-sized planetesimals requires $e < 0.01-0.03$ for snow but ices can grow if $e < 0.1$ provided the impactors are small.

Our results for the Kuiper belt are, generally speaking, in good agreement with Stern (1996a,b). They obtained that the condition for sustained growth of Kuiper belt objects in the range 50–180 km radius regime, is $e < 0.05-0.1$ if the objects are strong as ice, and $e < 0.02-0.05$ if they are mechanically weak like snow. Many of the detected objects have eccentricities that exceed these values, and are therefore likely to be suffering erosion and disruption today.

We may then conclude that either the primordial eccentricities in the Kuiper disk were much lower than what we observe today (e.g., Stern, 1996a,b), or primordial Kuiper belt objects with sizes higher than ~ 100 km were produced directly from small solid particles without experiencing accretion through intermediate sizes. In the second case, Kuiper belt objects observed today smaller than 100 km in radious would likely be collisional fragments of primordial larger objects.

5. Formation of large planetesimals by the accretion of small particles

We may then conclude from the previous that accretion requires a maximum impactor target mass ratio of $\sim 0.1-0.01$ during all the accretionary epoch at all locations in the disk to avoid disruption of the target. Here we investigate if planetesimals could be formed by accretion of small solid particles only.

The differential mass distribution of particles colliding with a planetesimal of mass m_t obey a power law number distribution, which is a function of the independent variable m' and two other parameters, K and q (e.g., Harris and Ward, 1982; Colwell, 1993, 1996):

$$dN(m') = n(m')dm' = Km'^{-q}dm'. \tag{4}$$

The functional form of Eq. (4) is valid up to mass m_M, which represents the largest size of particles present at any given time. Depending on the value of q the mass would be mostly contained in small ($q > 2$) or large ($q < 2$) particles (Safronov, 1969; Lissauer and Safronov, 1991; Benvenuto et al., 2009). The lower limit of the distribution is m_0, which represents the smallest size of particles present at any given time. It is usually assumed $m_0 = 0$ for $q < 2$ (e.g., Harris and Ward, 1982), while m_0 must be greater than zero for $q > 2$ to assure the convergence of Eq. (4) (e.g., Colwell, 1996; Showalter et al., 1992).

The growth rate of m_t due to the accretion of the whole distribution of particles is given by

$$\frac{dm_t}{dt}(m_M) = \int_{m_0}^{m_M} \pi(R+R')^2 v_r \left(1+\frac{v_e^2}{v_r^2}\right) m' n(m') dm', \tag{5}$$

where R and R' are the radius of m_t and m', respectively. v_r is the relative velocity between m_t and m' and v_e is the surface escape velocity. Assuming that the bulk density of m_t and m' are the same, Eq. (5) yields

$$\frac{dm_t}{dt}(m_M) = 3K\pi v_r \left(1+\frac{v_e^2}{v_r^2}\right)\left[R^2 \frac{(m_M^{(2-q)} - m_0^{(2-q)})}{(6-3q)} + 2R\frac{(R_M m_M^{(2-q)} - R_0 m_0^{(2-q)})}{(7-3q)} + \frac{(R_M^2 m_M^{(2-q)} - R_0^2 m_0^{(2-q)})}{(8-3q)}\right], \tag{6}$$

where R_M and R_0 are the radius of m_M and m_0, respectively.

The growth rate of m_t due to the accretion of particles having mass m_1 or smaller ($m_0 \le m_1 \le m_M$) is given by

$$\frac{dm_t}{dt}(m_1) = \int_{m_0}^{m_1} \pi(R+R')^2 v_r \left(1+\frac{v_e^2}{v_r^2}\right) m' n(m') dm', \tag{7}$$

$$\frac{dm_t}{dt}(m_1) = 3K\pi v_r \left(1+\frac{v_e^2}{v_r^2}\right)\left[R^2 \frac{(m_1^{(2-q)} - m_0^{(2-q)})}{(6-3q)} + 2R\frac{(R_1 m_1^{(2-q)} - R_0 m_0^{(2-q)})}{(7-3q)} + \frac{(R_1^2 m_1^{(2-q)} - R_0^2 m_0^{(2-q)})}{(8-3q)}\right], \tag{8}$$

where R_1 is the radius of m_1.

The probability of planetesimal growth from mass m_t to $m_t + dm_t$ being due to the accretion of particles having mass m_1 or smaller is given by

$$P(m_1) = \frac{(dm_t/dt)(m_1)}{(dm_t/dt)(m_M)}. \tag{9}$$

If $m_1 = m_M$, then $P(m_M) = 1$.

The growth time scale of m_t assuming that accretes particles of mass m_1 or smaller is defined as

$$\tau(m_1) = \frac{m_t}{(dm_t/dt)(m_1)}. \tag{10}$$

We introduce the growth delay factor $F(m_1)$ in the following form:

$$F(m_1) = \frac{\tau(m_1)}{\tau(m_M)} = \frac{(dm_t/dt)(m_M)}{(dm_t/dt)(m_1)} = \frac{1}{P(m_1)}. \tag{11}$$

If $m_1 = m_M$, then $\tau(m_1) = \tau(m_M)$ and $F(m_M) = 1$.

We replace in Eqs. (6) and (8) $m_M = \alpha m_t$, $m_1 = \epsilon m_M$ and $m_0 = \beta m_M$, obtaining

$$\frac{dm_t}{dt}(m_M) = 3K\pi v_r \left(1+\frac{v_e^2}{v_r^2}\right) R^2 \alpha^{(2-q)} m_t^{(2-q)} \times \left[\frac{(1-\beta^{(2-q)})}{(6-3q)} + \frac{2(\alpha^{1/3} - \beta^{(\frac{7}{3}-q)}\alpha^{1/3})}{(7-3q)} + \frac{(\alpha^{2/3} - \beta^{(\frac{8}{3}-q)}\alpha^{2/3})}{(8-3q)}\right], \tag{12}$$

$$\frac{dm_t}{dt}(m_1) = 3K\pi v_r \left(1+\frac{v_e^2}{v_r^2}\right) R^2 \alpha^{(2-q)} m_t^{(2-q)} \left[\frac{(\epsilon^{(2-q)} - \beta^{(2-q)})}{(6-3q)} + \frac{2(\epsilon^{(\frac{7}{3}-q)}\alpha^{1/3} - \beta^{(\frac{7}{3}-q)}\alpha^{1/3})}{(7-3q)} + \frac{(\epsilon^{(\frac{8}{3}-q)}\alpha^{2/3} - \beta^{(\frac{8}{3}-q)}\alpha^{2/3})}{(8-3q)}\right]. \tag{13}$$

Eqs. (9) and (11) were computed for $q = 1.6$, 1.8, 2.5, and 3 using Eqs. (12) and (13) for $\alpha =$ 0.01, 0.1, 1, $\epsilon =$ 0.01, 0.1 and $\beta = 10^{-3}, 10^{-4}, 10^{-5}$. The results of Eqs. (9) and (11) are shown in Table 1 for $q = 1.6$, Table 2 for $q = 1.8$, Table 3 for $q = 2.5$ and Table 4 for $q = 3$.

Table 1
Probability $P(m_1)$ and delay factor $F(m_1)$ of the growth of a planetesimal of mass m_t due to the accretion of particles of mass m_1 or smaller for $q=1.6$. m_t is immersed in a swarm of particles with masses in the range $m_0 < m_1 < m_M$. $m_M = \alpha m_t$, $m_1 = \epsilon m_M$ and $m_0 = \beta m_M$.

α	β	ϵ	P	F
0.01	10^{-5}	0.01	0.12604	7.9339
0.01	10^{-5}	0.10	0.34851	2.8694
0.01	10^{-4}	0.01	0.11511	8.6871
0.01	10^{-4}	0.10	0.34036	2.9381
0.01	10^{-3}	0.01	0.08591	11.640
0.01	10^{-3}	0.10	0.31859	3.1388
0.1	10^{-5}	0.01	0.10543	9.4851
0.1	10^{-5}	0.10	0.30975	3.2284
0.1	10^{-4}	0.01	0.09649	10.364
0.1	10^{-4}	0.10	0.30286	3.3019
0.1	10^{-3}	0.01	0.07235	13.822
0.1	10^{-3}	0.10	0.28423	3.5182
1	10^{-5}	0.01	0.07666	13.044
1	10^{-5}	0.10	0.25314	3.9505
1	10^{-4}	0.01	0.07054	14.176
1	10^{-4}	0.10	0.24818	4.0293
1	10^{-3}	0.01	0.05355	18.675
1	10^{-3}	0.10	0.23444	4.2655

Table 2
The same as in Table 1 for $q=1.8$.

α	β	ϵ	P	F
0.01	10^{-5}	0.01	0.29089	3.4378
0.01	10^{-5}	0.10	0.54050	1.8501
0.01	10^{-4}	0.01	0.24934	4.0106
0.01	10^{-4}	0.10	0.51358	1.9471
0.01	10^{-3}	0.01	0.17109	5.8450
0.01	10^{-3}	0.10	0.46287	2.1604
0.1	10^{-5}	0.01	0.25298	3.9529
0.1	10^{-5}	0.10	0.49258	2.0301
0.1	10^{-4}	0.01	0.21655	4.6180
0.1	10^{-4}	0.10	0.46783	2.1375
0.1	10^{-3}	0.01	0.14838	6.7394
0.1	10^{-3}	0.10	0.42153	2.3723
1	10^{-5}	0.01	0.19428	5.1473
1	10^{-5}	0.10	0.41527	2.4081
1	10^{-4}	0.01	0.16657	6.0033
1	10^{-4}	0.10	0.39517	2.5306
1	10^{-3}	0.01	0.11466	8.7213
1	10^{-3}	0.10	0.35749	2.7973

Table 3
The same as in Table 1 for $q=2.5$.

α	β	ϵ	P	F
0.01	10^{-5}	0.01	0.96727	1.0338
0.01	10^{-5}	0.10	0.99129	1.0088
0.01	10^{-4}	0.01	0.89822	1.1133
0.01	10^{-4}	0.10	0.97292	1.0278
0.01	10^{-3}	0.01	0.68469	1.4605
0.01	10^{-3}	0.10	0.91611	1.0916
0.1	10^{-5}	0.01	0.96216	1.0393
0.1	10^{-5}	0.10	0.98894	1.0112
0.1	10^{-4}	0.01	0.88544	1.1294
0.1	10^{-4}	0.10	0.96652	1.0346
0.1	10^{-3}	0.01	0.66130	1.5122
0.1	10^{-3}	0.10	0.90101	1.1099
1	10^{-5}	0.01	0.95028	1.0523
1	10^{-5}	0.10	0.98320	1.0171
1	10^{-4}	0.01	0.85768	1.1659
1	10^{-4}	0.10	0.95191	1.0505
1	10^{-3}	0.01	0.61588	1.6237
1	10^{-3}	0.10	0.87020	1.1492

Table 4
The same as in Table 1 for $q=3$.

α	β	ϵ	P	F
0.01	10^{-5}	0.01	0.99889	1.0011
0.01	10^{-5}	0.10	0.99989	1.0001
0.01	10^{-4}	0.01	0.98905	1.0111
0.01	10^{-4}	0.10	0.99888	1.0011
0.01	10^{-3}	0.01	0.89402	1.1185
0.01	10^{-3}	0.10	0.98918	1.0109
0.1	10^{-5}	0.01	0.99874	1.0013
0.1	10^{-5}	0.10	0.99986	1.0001
0.1	10^{-4}	0.01	0.98781	1.0123
0.1	10^{-4}	0.10	0.99861	1.0014
0.1	10^{-3}	0.01	0.88627	1.1283
0.1	10^{-3}	0.10	0.98703	1.0131
1	10^{-5}	0.01	0.99839	1.0016
1	10^{-5}	0.10	0.99978	1.0002
1	10^{-4}	0.01	0.98502	1.0152
1	10^{-4}	0.10	0.99796	1.0020
1	10^{-3}	0.01	0.87033	1.1490
1	10^{-3}	0.10	0.98232	1.0180

5.1. Before runaway growth

Before the stage of runaway growth, we may assume $m_t \sim m_M$ ($\alpha = 1$). The maximum mass m_1 accreted by m_t must be less than 0.1–0.01 m_t to avoid disruption of m_t. For $q = 1.8$ and 1.6, the probability of growth of m_t due to accretion of bodies smaller than 0.1–0.01 m_t is $P \sim 0.1-0.4$ while the time scale of growth of m_t is increased $\sim 2-18$ times with respect to the case in which m_t accretes mass from the whole distribution of particles (see Tables 1 and 2). For $q > 2$, the probability of growth of m_t due to accretion of bodies smaller than 0.1–0.01 m_t is $P \sim 0.7-1$ while the time scale of growth of m_t remains almost unchanged with respect to the case in which m_t accretes mass from the whole distribution of particles (see Tables 3 and 4). We may then conclude that during the first step of the accretionary epoch, q must be greater than 2. This result is consistent with the definition given by Kokubo and Ida (2000). They defined the growth mode that produces a power-law mass distribution with $q > 2$ as runaway growth, i.e., most mass of the system exists in small bodies, while the largest body becomes more massive and is detached from the distribution.

5.2. After runaway growth: oligarchic growth

Wetherill and Stewart (1993) studied the evolution of the planetesimal system that evolved only through collisions and fragmentation. They found that planetesimals mass distribution relaxes to a piecewise power law: a population of small planetesimals due to fragmentation with $q \sim 1.7$, and a population of large planetesimals that follow an accretive regime with $q \sim 2.5$ which, in turn, contained most of the mass of the system. Kenyon and Bromley (2004a,b, 2005) and Stern and Colwell (1997) found a similar bimodal mass distribution for the late stages of planet formation.

During oligarchic growth m_t represents any mass of the distribution of large bodies which accretes particles from the distribution of small planetesimals. Small planetesimals could follow an inverse power law with $q \sim 1.6-1.8$. Looking at Tables 1 and 2, m_1 should be $\sim m_M$ for these values of q since otherwise, the probability $P(m_1)$ would turn very low. Since m_t must accrete bodies smaller than 0.1–0.01 m_t to avoid disruption, we may then conclude that the upper limit m_M of the distribution of small particles for $q<2$ must be smaller than 0.1–0.01 m_t for all m_t. Thus, the main result is that the upper limit m_M of the distribution of small bodies must be smaller than 0.1–0.01 times the lower limit m_0 of the distribution of large bodies unless the index q of the distribution of small particles were greater than 2.

Actually, accretion among bodies of the distribution of large planetesimals during oligarchic growth is a matter of debate. Let's suppose that m_t may accrete bodies from such distribution. Although the bodies accreted by m_t must be smaller than 0.1–0.01 m_t to avoid disruption, this does not represent a problem provided $q>2$, which means that the probability that m_t accretes planetesimals smaller than 0.1–0.01 m_t turns high.

6. Conclusions

We have shown that accretion requires very low eccentricities during all the accretionary epoch at all locations throughout the disk. Since it seems to be difficult to achieve, a large population of planetesimals with radius higher than 100 km were probably produced directly from small solid particles without experiencing accretion through intermediate sizes. We then conclude that large planetesimals are formed either invoking modern scenarios of gravitational instability (Johansen et al., 2007; Youdin and Goodman, 2005) or by accreting small bodies only. We obtain that during all the accretionary epoch, planetesimals growth requires an impactor target mass ratio smaller than 0.1–0.01 at all locations. This implies that the exponent q of the power law mass distribution of bodies must be greater than 2 during all the planetary formation process. However, if during oligarchic growth a bimodal mass distribution of small and large bodies exists, the mass distribution of small bodies allows $q<2$ provided the largest mass of such distribution were at least one or two orders of magnitude lower than the smallest mass of the distribution of large planetesimals.

Acknowledgments

We are thankful to the anonymous referees for critically reading this paper and also for many constructive comments. This research was supported by Intituto Argentino de Radioastronomía IAR-CONICET and by CONICET grant PIP 112-200901-00461, Argentina.

References

Asphaug, E., Ryan, E.V., Zuber, M.T., 2002. Asteroid interiors. In: Bottke, W.F., Cellino, R.P., Paolicchi, P., Binzel, R.P. (Eds.), Asteroids III. Univ. of Arizona Press, Tucson, pp. 463–484.

Benvenuto, O.G., Fortier, A., Brunini, A., 2009. Forming Jupiter, Saturn, Uranus and Neptune in few millon years by core accretion. Icarus 204, 752–755.

Benz, W., 2000. Low velocity collisions and the growth of planetesimals. In: Benz, W., Kallenbach, R., Lugmair, G.W. (Eds.), From Dust to Terrestrial Planets. Kluwer Academic, Dordrecht, pp. 279–300.

Bizzarro, M., Baker, J.A., Haack, H., Lundgaard, K.L., 2005. Rapid timescales for accretion and melting of differentiated planetesimals inferred from ^{26}Al ^{26}Mg chronometry. The Astrophysical Journal 632, L41–L44.

Blum, J., et al., 2000. Growth and form of planetary seedlings: results from a microgravity aggregation experiment. Physical Review Letters 85, 2426–2429.

Bottke, W.F., Nolan, M.C., Greenberg, R., Kolvoord, R.A., 1994. Velocity distributions among colliding asteroids. Icarus 107, 255–268.

Bottke, W.F., Durda, D.D., Nesvorny, D., Jedicke, R., Morbidelli, A., Vokrouhlicky, D., Levison, H., 2005. The fossilized size distribution of the main asteroid belt. Icarus 175, 111–140.

Colwell, J.E., 1993. Power-law confusion: you say incremental, I say differential. In: 24th Lunar and Planetary Science Conference, Houston, TX, pp. 325–326.

Colwell, J.E., 1996. Size distributions of circumplanetary dust. Advances in Space Research 17, 12.161–12.170.

Davis, D.R., Weidenschilling, S.J., Farinella, P., Paolicchi, P., Binzel, R.P., 1989. Asteroids collisional history—effects on sizes and spins. In: Asteroids II. Tucson, AZ. University of Arizona Press, CNR and MPI Supported Research, pp. 805–826.

Farinella, P., Davis, D.R., 1992. Collision rates and impact velocities in the main asteroid belt. Icarus 97, 111–123.

Farinella, P., Davis, D.R., 1996. Short-period comets: primordial bodies or collisional fragments?. Science 273, 938–941.

Goldreich, P., Ward, W.R., 1973. The formation of planetesimals. The Astrophysical Journal 183, 1051–1062.

Goldreich, P., Lithwick, Y., Sari, R., 2004. Planet formation by coagulation: a focus on Uranus and Neptune. Annual Review of Astronomy and Astrophysics 42, 549–601.

Harris, A.W., Ward, W.R., 1982. Dynamical constraints on the formation and evolution of planetary bodies. Annual Review of Earth and Planetary Sciences 10, 61–107.

Ida, S., Makino, J., 1992. N-body simulation of gravitational interaction between planetesimals and a protoplanet I. Velocity distribution of planetesimals. Icarus 96, 107–120.

Ida, S., Guillot, T., Morbidelli, A., 2008. Accretion and destruction of planetesimals in turbulent disks. The Astrophysical Journal 686, 1292–1301.

Inaba, S., Tnaka, H., Nakazawa, K., Wetherill, G.W., Kokubo, E., 2001. High-accuracy statistical simulation of planetary accretion: II. Comparison with N-body simulation. Icarus 149, 235–250.

Johansen, A., Oishi, J.S., Mac Low, M.-M., Klahr, H., Henning, T., Youdin, A.N., 2007. Rapid planetesimal formation in turbulent circumstellar disks. Nature 448, 1022–1025.

Johansen, A., Youdin, A.N., Klahr, H., 2009. Zonal flows and long-lived axisymmetric pressure bumps in magnetorotational turbulence. The Astrophysicals Journal 697, 1269–1289.

Johansen, A., Youdin, A.N., Lithwick, Y., 2012. Adding particle collisions to the formation of asteroids and Kuiper belt objects via streaming instabilities. Astronomy and Astrophysics 537, A125.

Kenyon, S.J., Bromley, B.C., 2004a. Collisional cascades in planetesimal disks. II. Embedded planets. The Astrophysical Journal 127, 513–530.

Kenyon, S.J., Bromley, B.C., 2004b. The size distribution of Kuiper belt objects. The Astrophysical Journal 128, 1916–1929.

Kenyon, S.J., Bromley, B.C., 2005. Prospects for detection of catastrophic collisions in debris disks. The Astrophysical Journal 130, 269–279.

Kobayashi, H., Tanaka, H., Krivov, A.V., Inaba, S., 2010. Planetary growth with collisional fragmentation and gas drag. Icarus 209, 836–847.

Kokubo, E., Ida, S., 2000. Formation of protoplanets from planetesimals in the Solar Nebula. Icarus 143, 15–27.

Lissauer, J.J., Safronov, V.S., 1991. The random component of planetary rotation. Icarus 93, 288–297.

Lissauer, J.J., Stewart, G.R., 1993. Growth of planets from planetesimals. In: Protostars and Planets III, pp. 1061–1088.

Manley, S.P., Migliorini, F., Bailey, M.E., 1998. An algorithm for determining collision probabilities between small Solar System bodies. Astronomy and Astrophysics Supplement Series 133, 437–444.

Morbidelli, A., Bottke, W.F., Nesvorny, D., Levison, H.F., 2009. Asteroids were born big. Icarus 204, 558–573.

Nakagawa, Y., Hayashi, C., Nakazawa, K., 1983. Accumulation of planetesimals in the solar nebula. Icarus 54, 361–376.

Ohtsuki, K., Stewart, G., Ida, S., 2002. Evolution of planetesimal velocities based on three-body orbital integrations and growth of protoplanets. Icarus 155, 436–453.

Paszun, D., Dominik, C., 2009. Collisional evolution of dust aggregates. From compaction to catastrophic destruction. Astronomy and Astrophysics 507, 1023–1040.

Safronov, V., 1969. Evolution of the Protoplanetary Cloud and the Formation of the Earth and Planets, Nauka, Moscow. NASA TTF-677, US Government Printing Office, Washington, DC, 1972.

Showalter, M.R., Pollack, J.B., Ockert, M.E., Doyle, L.R., Dalton, B., 1992. A photometric study of saturn's F ring. Icarus 10, 394–411.

Stern, S.A., 1996a. Signatures of collisions in the Kuiper Disk. Astronomy and Astrophysics 310, 999–1010.

Stern, S.A., 1996b. The primordial Kuiper Disk. The Astronomical Journal 112, 1203–1211.

Stern, S.A., Colwell, J.E., 1997. Accretion in the Edgeworth-Kuiper belt: forming 100–1000 km radius bodies at 30 AU and beyond. The Astrophysical Journal 114, 841–848.

Stevenson, D.J., Harris, A.W., Lunine, J.J., 1986. Origin of satellites. In: Satellites. University of Arizona Press, Tucson, AZ. NASA-Supported Research, pp. 39–88.

Thommes, E.W., Duncan, M.J., Levison, H.F., 2003. Oligarchic growth of giant planets. Icarus 161, 431–455.

Tsiganis, K., Gomes, R., Morbidelli, A., Levison, H.F., 2005. Origin of the orbital architecture of the giant planets of the Solar System. Nature 435, 459–461.

Weidenschilling, S.J., 1980. Dust to planetesimals: settling and coagulation in the solar nebula. Icarus 44, 172–189.
Weidenschilling, S.J., 1997. The origin of comets in the solar nebula: an unified model. Icarus 127, 290–306.
Weidenschilling, S.J., Spaute, D., Davis, D.R., Marzari, F., Ohtsuki, K., 1997. Accretional evolution of a planetesimals swarm. Icarus 128, 429–455.
Weidenschilling, S.J., 2011. Initial sizes of planetesimals and accretion of the asteroids. Icarus 214, 671–684.
Wetheril, G.W., Stewart, G.R., 1993. Formation of planetary embryos: effects of fragmentation, low relative velocity, and independent variation of eccentricity and inclination. Icarus 106, 190–209.
Youdin, A.N., Goodman, J., 2005. Streaming instabilities to protoplanetary disks. The Astrophysical Journal 620, 459–469.